P1.15

AN OBSERVATIONAL ANALYSIS OF AN ALABAMA DRYLINE EVENT ON MARCH 19- 20, 2003

R.E. Barbré, Jr., J. Mecikalski, K. Knupp, W. Mackenzie, Jr, P. Gatlin, D. Phillips
University of Alabama at Huntsville, Huntsville, Alabama

1. INTRODUCTION

Drylines are prevalent features across the Southern Great Plains during the springtime months. The high terrain of the Rocky Mountains and High Plains, combined with the upper air pattern over this region, provide a favorable environment for dry air aloft to mix to the surface. Drylines progress eastward during the day through vertical mixing (Schaefer, 1973) as the surface layer heats and erodes the radiation inversion, but they usually stall before reaching the longitude of the TX/ LA border. The increasingly lower surface elevation across the Southern Plains deepens the boundary layer, and thus requires more heating to eliminate the inversion. The dryline retrogrades during the evening hours as the surface cools and mixing is further inhibited (McCarthy and Koch, 1981). Drylines are areas for moisture convergence at lower levels, which aid to the initiation of convection in the Southern Plains. In rare cases, drylines can form farther east in the southeast region of the United States. Although it must travel much farther, downsloping air advecting from the Mexican Plateau travels over the Gulf of Mexico and mixes down to the surface with the aid of a turbulent boundary layer. Under synoptically active conditions, the dryline usually extends toward the equator from a low pressure area along a frontal zone (Hane et. al. 2001).

On 19 Mar 2003, a vigorous occluded cyclone was propagating across the central United States, bringing part of an unusually plume of dry air northeastward into the southeast United States. In addition, the dynamics for storm development were very favorable in the warm sector. The dryline that formed over AL on this day provided a boundary and an area of low-level moisture convergence for storms to initiate. Ahead of the dryline, southerly winds prevailed across the region, bringing 21° C dewpoints northward from the Gulf of Mexico. In addition to the moisture convergence ahead of the dryline, lift along the warm front helped initiate convective activity in GA and in the FL Panhandle. These boundaries, combined with the strong dynamics, enabled severe storms and tornadoes to develop across this region. Nine tornadoes were reported in AL, seven in GA, four in FL, and two in TN. In addition, hail up to 2.75 inches in diameter, and wind speeds of 30 ms^{-1} were reported. Eleven deaths, numerous injuries, and two missing people resulted from this event (SPC 2003).

The purpose of this paper is to provide synoptic and point analyses of this undocumented atmospheric phenomenon and to discuss its attributes. Reasons for the dryline passage will be discussed through a synoptic and skew-T overview. The satellite and radar section will further explain dryline passage as well as the initiation and persistence of storms. Finally, the MIPS section will discuss in detail the conditions in Huntsville, AL and Camp Adahi, GA during this event.

2. OBSERVATIONAL DATA SOURCES

Using maps, soundings, satellite, Weather Surveillance Radar (WSR- 88D), and instruments from the MIPS from the University of Alabama in Huntsville (UAH), this event was recorded and studied. Synoptic weather maps and radiosonde measurements from 1200 UTC 19 Mar to 0000 UTC 21 Mar were used along with satellite imagery, data from the MIPS instruments, and radar images and loops from the KBMX, KHTX, KMRX, KMXX, and KOHX WSR-88D radars. The MIPS system was located in Camp Adahi, GA (34.63 N, -85.48 W) and was equipped with a 915 MHz Doppler profiler and a CT-25K celiometer. The 12 channel microwave profiling radiometer was located on the roof of the National Space and Science Technology Center (NSSTC) in Huntsville, AL. Datasets from all of these instruments were used. Since Camp Adahi is located about 101 km southeast of Huntsville, data from the radiometer differs from data from the other MIPS instruments, specifically while the dryline was located between the NSSTC and Camp Adahi.

3. SYNOPTIC SET-UP

The synoptic weather pattern for 19 Mar 2003 created an active weather situation for the Southeast while simultaneously advecting dry air from the Mexican Plateau into the region. The original source was an extremely large region of

dry air across the Tropical Pacific, extending from the equator to about 35° N. A HYSPLIT (HYbrid Single-Particle Lagrangian Integrated Trajectory) model run (Fig. 1) shows that dry air from 100 dm, 150 dm, and 250 dm above ground level (AGL) was also being advected into the Southeast from the northern Mexican Plateau. A turbulent boundary layer over AL was able to transport the dry air down to the surface as shown for Great Plains drylines in Crawford and Bluestein (1996).

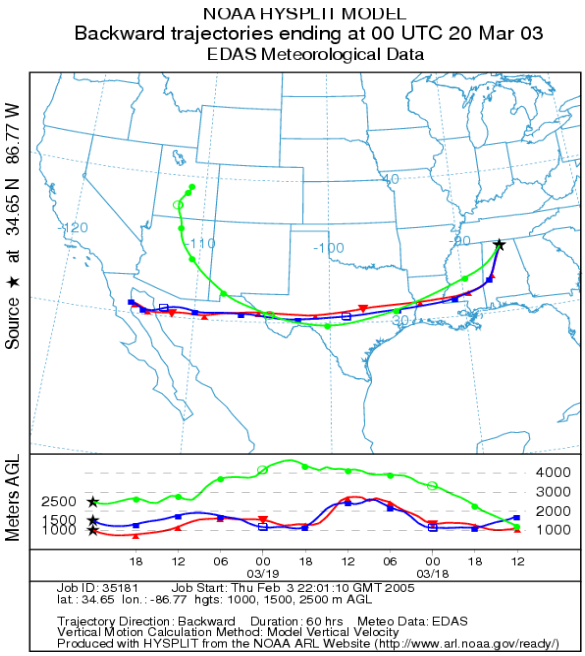

Fig. 1: HYSPLIT back trajectories for parcels at 100 dm (red), 150 dm (blue), and 250 dm (green) from March 17th at 1200 UTC to March 20th at 0000 UTC.

The 1200 UTC 300 hPa analysis on the 19 Mar shows a closed 906 dm low located in northern TX within a broad ridge across North America. A subtropical jet maximum of 65 ms^{-1} existed over southeast TX. East of the low center, strong diffluence existed over AL and MS. A more pronounced ridge also existed off of the New England Coast. A shortwave at 500 hPa containing a 26- unit vortictiy maximum was propagating through TN and, along with winds of 50 ms^{-1} at the same level, was providing the Southeast with strong positive vorticity advection (PVA). Drier air at this level was concentrated south of the low height center in TX and Mexico, and the strong southwesterly winds advected the drier air over the Southeast United States. The dry air at 500 hPa is depicted in Fig.2 by the 24° C dewpoint difference between Nashville, TN and Birmingham, AL, with readings of -19° C and -43° C respectively.

At 700 hPa, omega values were under -16 Pa $(s)^{-1}$ across northern AL and TN and a secondary minimum of under -10 $Pa(s)^{-1}$ developed over LA. These low omega values were supported by the differential PVA up to 500 hPa and by the warm air advection (WAA) shown on the 850 hPa map. By the omega equation, both of these processes lead to synoptic scale upward motion. In addition to the WAA at 850 hPa, moist air, with dewpoint depressions of only 1° C to 2° C, was being advected over the eastern Atlantic Ocean and into the deep Southeast by a high in the Caribbean. However, Slidell, LA (KLIX) was experiencing a dewpoint depression of 26° C as the drier air from the Mexican Plateau had already passed the region at this level. A southwest wind at 850 hPa advected this drier air into AL. In addition to the strong dewpoint gradient between KLIX and KBHM, a significant cyclonic wind shift and a wind acceleration developed near the MS/ AL border, causing a pressure trough in the warm sector of the mid- latitude cyclone. The 925 hPa chart depicts the wind shift in addition to a strong dewpoint gradient ahead of it. These two factors caused strong moisture convergence across the Southeast and the dryline that developed provided a lifting mechanism for the moist air to the east.

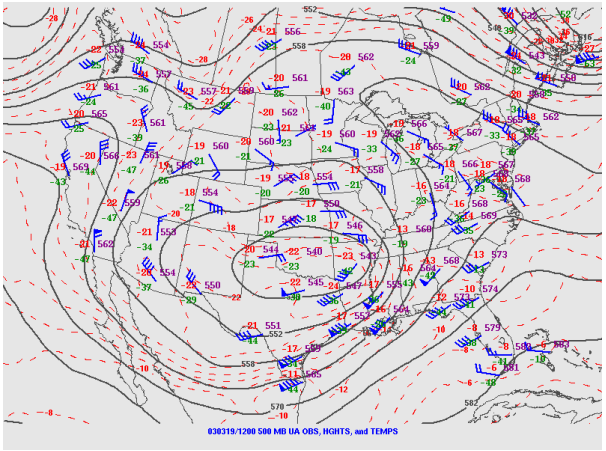

Fig. 2: 500 hPa isohypses, isotherms, and observations for the Continental US and Canada. Isohypses are black solid lines and isotherms are red dashed lines.

Surface charts from the 19 Mar from 1416 UTC to 1816 UTC also show a cyclonic wind shift across AL and a dewpoint gradient starting to develop. In this case, the kinematic dryline lagged behind the thermodynamic dryline, similar to cases in the Southern Plains. Fig. 3 shows the leading edge of the dewpoint gradient ahead of the wind shift and is consistent with Fig.1 in Shaw et al. (1996), which shows a dryline at the TX/ NM border. KHSV had a higher surface dewpoint (17°

C) at 1416 UTC than observations in both MS and GA. This also suggests that moist air from the Gulf of Mexico was converging in AL. The dewpoint at KHSV dropped 5° C in three hours as the dryline passed. The dryline stretched from north of KBNA to the Gulf Coast, with dewpoints dropping to 2° C at KMOB. Calm winds kept dewpoints low at KMOB, as other stations on the Gulf Coast were experiencing light offshore winds, causing dewpoints to remain near 10° C west of the dryline.

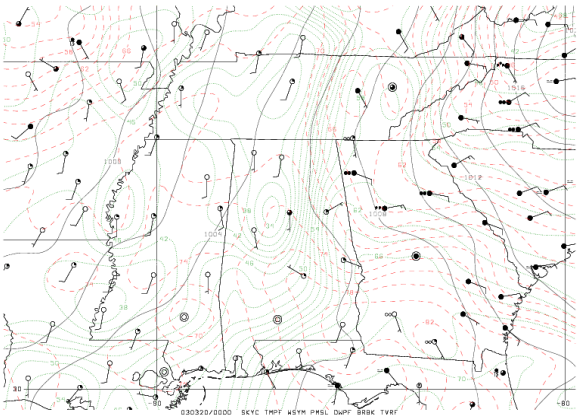

Fig. 3: Surface Analysis from March 20th, at 0000 UTC showing wind plots and contours of pressure, dewpoint, and virtual temperature. The ridging of virtual temperature in AL indicates warmer, drier air behind the dryline located in eastern AL. An enhanced virtual temperature gradient in GA and SC shows the density change associated with CAD. The wind shift from east- southeasterly to southerly occurs after the leading edge of the dewpoint gradient passes.

Overnight, rain- cooled air and the diurnal temperature cycle contributed to the weakening of the temperature and moisture gradients across AL. This caused the dryline to retrograde into western AL and eventually erode overnight at the surface. On 20 Mar, the same basic synoptic conditions prevailed over the Southeast, with two main surface features across the United States: an occluded cyclone in the Southern Plains, which had weakened to 999 hPa from 991 hPa on 19 Mar, and a 1029 hPa anticyclone in the Northeast, which induced CAD east of the Appalachians. The dammed air then flowed south along the mountains and eventually drained into the northern parts of GA and AL. Strong divergence at 300 hPa still existed over the Southeast along with the continued progression of shortwave troughs from the positively tilted 500 hPa trough in TX. WAA persisted and a strong moisture gradient once again developed, aiding synoptic scale lifting and the redevelopment of the dryline respectively. On both days, the combination of the synoptic weather pattern and the existence of the dryline provided a favorable environment for severe storms to develop.

Severe storms developed during the day on 19 Mar, progressed eastward and merged into squall lines in GA and SC on the 20 Mar. Stations ahead of the dryline reported low- level veering and jet maxima of up to 75 ms^{-1}. Soundings from KJAX, KCHS, and KGSO suggest that the environment ahead of the dryline was favorable for storms to continue since an abundance of moisture and shear was in place at these locations. Strong frontal inversions at KJAX, KFFC, KGSO, and KCHS showed that these stations were experiencing CAD. By the afternoon on 20 Mar, storms had outrun the dryline, and were moving rapidly towards the Atlantic Coast. Again, storms formed in AL along the reformed dryline.

The Storm Prediction Center (SPC) in Norman, OK issued convective outlooks for this region. On 19 Mar, only a slight risk was issued for days one and two. On day one, the slight risk area had a sharp boundary just east of the approximate dryline location through central AL. All outlooks had a sharp probability gradient in the vicinity of the forecasted location of the dryline. On 20 Mar, a moderate risk was issued for southeast GA, FL, and SC, and the slight risk area extended into the Ohio Valley. The close proximity in AL of the boundaries for all products issued by the SPC shows that a synoptic scale boundary existed through central AL in which storms were initiating to the east and the weather was relatively calm to the west.

Several studies (Parsons et al. 1990, Peckham and Wicker 1999, Shaw et al. 1996, Ziegler and Hane 1992, and Sun and Wu 1991) have shown conflicting correlations between the virtual potential temperature gradient and the dryline location. Fig. 4 shows that, for this case, a strong correlation existed between the virtual potential temperature gradient and the dryline location in the morning. However, no correlation existed after about 1300 UTC on both days. Since virtual potential temperature indicates density, the inconsistent correlation could possibly be attributed to mixing ahead of the dryline combined with surface heating. Mixing would lessen the moisture contrast by transporting drier air down from immediately above the surface ahead of the dryline. In addition, surface heating ahead of the dryline during the day would lessen the temperature difference across the dryline. Both of these processes would lessen the density difference across the dryline. Despite these processes, the virtual temperature gradient persisted longer to the south. Southerly winds

were bringing warm, moist air from the Gulf of Mexico, and the air behind the dryline and near the coast was not as warm as the same air farther north since the cold air drainage did not affect locations southwest of Montgomery, AL. In addition, locations on the coast would be moister ahead of the dryline given their proximity to a large water source. Thus, a greater density difference would exist to the south and the virtual potential temperature gradient would better coexist with the dryline. A density difference across the dryline is not as apparent as a density difference caused by CAD or a cold front, both of which were shown during this study to have a much better correlation between the dewpoint and virtual temperature gradient.

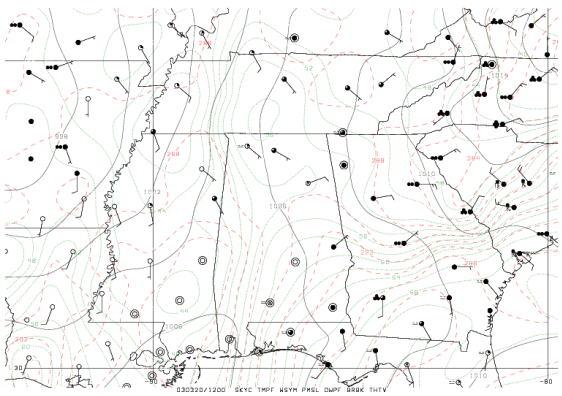

Fig. 4: Surface Analysis from March 20th, at 1200 UTC showing wind plots and contours of pressure, dewpoint, and virtual potential temperature. In this case, the virtual potential temperature gradient coexisted with the dryline in the morning, but showed no association with the dryline in the afternoon. The cold air drainage off of the Piedmont is depicted by the strong virtual potential temperature gradient throughout GA and SC.

4. SOUNDINGS

In order to get a good representation of the environment across northern AL on 19 Mar, soundings from KBNA, KBMX, and KFFC were examined. The 1200 UTC 19 Mar sounding at KBNA appears to be corrupted by precipitation as the atmosphere is moist throughout and winds back at lower levels, indicating cold air advection (CAA). However, it depicts a 55 ms^{-1} jet maximum at 300 hPa. The KFFC sounding also shows this jet maximum as well as a LLJ of 20 ms^{-1}. In addition, strong WAA is depicted at KFFC as the winds veer considerably with height at lower levels. The atmosphere is nearly saturated up to about 850 hPa, and then the dewpoint drops above a frontal inversion caused by cold air drainage from the Piedmont. The sounding shows a near dry adiabatic lapse rate in a layer from about 725 hPa to 675 hPa, which would help parcels that reach this level rise even farther and thus aid deep convection.

The curved hodographs of KFFC and KBMX and helicity values exceeding 700 m^2s^{-2} indicate very strong low- level wind shear and a potential for tornadoes. In addition to the strong low- level veering of winds, the KBMX sounding (Fig. 5) also depicts a dry adiabatic lapse rate from 650 hPa to 550 hPa and the low- level moisture converging into the region just ahead of the dryline.

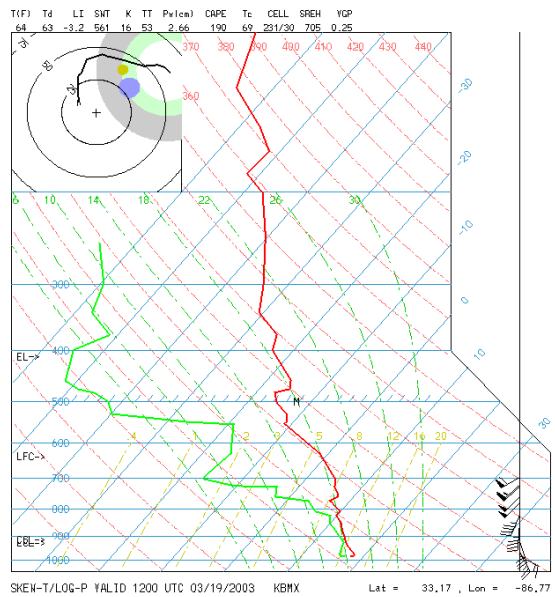

Fig. 5: Sounding from KBMX on March 19th, 2003 at 1200 UTC. Temperature and dewpoint profiles are denoted by red and green solid lines, respectively. At this time, moisture existed above a shallow radiation inversion up to about 770 hPa. This moisture combined with strong veering and the presence of the dryline helped to initiate storms in this region.

The cold air drainage did not reach KBMX at the time of the observation so the frontal inversion is not depicted. Only a weak capping inversion existed over the KBMX, but the atmosphere above 750 hPa remained dry as water vapor is concentrated near the surface. Due to the weak capping inversion, increased surfaced- based convective available potential energy (CAPE) in the warm sector, and the low- level moisture convergence, the region around KBMX was more favorable for early development of storms.

5. SATELLITE AND RADAR DATA

Visible satellite imagery from 19 Mar clearly shows the location of the dryline due to a sharp cloud line migrating across AL. Convection in GA

induced gravity waves ahead of the dryline. These gravity waves intersected with the dryline and aided in the development of Cumulonimbus clouds in northeast AL and TN. Their initiation spread towards the south- southwest as the day continued. The cloud line also began to develop a northeast to southwest orientation. However, training caused the continued development of storms across northeast AL and central TN through 2000 UTC. Storms continued to intensify towards the south as depicted by infrared satellite imagery showing cloud tops cooling in AL and GA. By 1800 UTC, the main areas of intense storms had merged and started to become less linear.

Fig. 6 shows the gravity waves ahead of the dryline and wave- like cloud features developing in MS and western AL behind the dryline. These cloud features, located about 4000 m above ground level (AGL) and oriented perpendicular to the wind field at this level, developed around 1900 UTC and were probably caused by gravity waves as well. These gravity waves were located below the exit region of the 300 hPa jet streak, which Uccellini and Koch (1986) describe as being a source for gravity waves due to geostrophic adjustment processes. In addition, the environment depicted by the KJAN sounding at 0000 UTC 20 Mar (Fig. 7) shows a "critical level" of enhanced saturation at approximately 600 hPa, along with a temperature inversion at 450 hPa and 22.5 ms^{-1} speed shear from 500 hPa to 300 hPa. This situation is conducive for ducting, as described in Lindzen and Tung (1976) as a maintenance mechanism, preventing gravity waves from losing energy to space and thus enabling them to propagate horizontally. These waves caused strong turbulence behind the dryline as 28 ms^{-1} winds at this level were experiencing opposite vertical motions over about 30 km across MS and AL. The gravity waves propagating through this region were able to aid in lifting parcels high enough to form clouds.

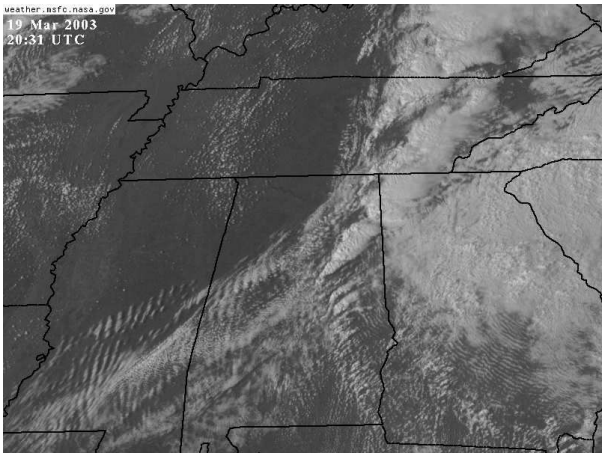

Fig. 6: Visible satellite image from March 19th at 2031 UTC. The dryline can be seen through TN and central AL. Storms have initiated just to the east of the dryline. HCRs can be seen ahead of the dryline in GA and wavelike cloud features exist behind the dryline in MS and western AL.

Water Vapor imagery (not shown) shows a dry filament extending into LA and MS from the drier air south of the upper- level low height center. Tollerud et. al. (2002) found a similar trait for drylines in the Southern Plains where a dry filament extends meridionally just west of the dryline. These filaments represent the dry air that has mixed to the surface with the aid of a turbulent boundary layer. The filament shown in the water vapor imagery for this day was not as pronounced as the filaments shown in Tollerud et. al. (2002), but it coincided with the dryline location in a similar manner.

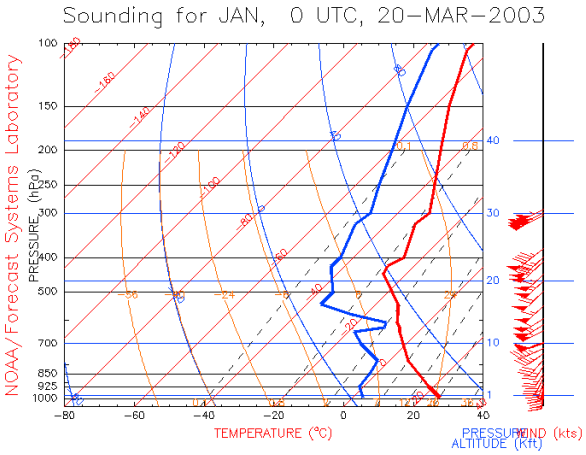

Fig. 7: Sounding for KJAN at 0000 UTC on March 20th. Temperature and dewpoint profiles are indicated by red and green lines, respectively. The enhanced moisture at ~600 hPa, speed shear, and the existence of a temperature inversion initiated and maintained gravity waves, which were propagating across MS during and prior to this time.

Satellite imagery shows a similar pattern for the next day. The boundary is still oriented northeast to southwest with isolated storms ahead of it in GA. In this region, HCRs persisted ahead of the dryline, which could have been responsible for initiating storms. Just before 1000 UTC 20 Mar, isolated storms developed near the intersection of HCRs and the dryline in southeast AL and southern GA. One of these storms spawned a deadly tornado in Camilla, GA, which damaged many homes and injured over 200 people. The intense storms progressed into the eastern parts of GA and into the Carolinas.

Radar imagery was taken from the WSR- 88D's out of KBMX, KHTX, KMRX, KOHX, and KMXX.

The C and S- shaped zero isodop in the velocity imagery (Fig. 8a) show both warm advection and confluence occurring in northern AL and southern TN on a relatively small scale, making the environment more favorable for convection in this region. On 19 Mar, animations from multiple stations, especially in AL, show the training of storms as they initiated in the same location and moved rapidly toward the northeast. Reflectivity imagery from KHTX at 1903 UTC 19 Mar (Fig. 8b) shows the storms initiating as individual cells in central and western AL and TN, just east of the dryline boundary. This follows Ziegler et. al. (1996), which showed that convection usually initiates between 10 and 20 km east of the dryline.

These individual storms merged into squall lines near KOHX. Another line of storms developed along a boundary intersecting with the dryline and extended northeast from 30 km north of KBMX. Since this boundary was oriented nearly perpendicular to the wind, it was able to provide enough lift to initiate storms. A weak line echo wave pattern can be seen from the KHTX radar at 1300 UTC. The slight undulations over central and southern TN and extreme northern AL indicate the presence of very strong winds in these isolated areas. The most intense storm was 77 dBZ in northern GA and was observed by the KHTX radar. Hail probably contributed to the very high dBZ values since reports of up to golfball- size hail came from this region. KHTX also picked up waves that appeared in the visible satellite imagery, but the waves could not be seen close to the radar. This could be explained by the radar beam passing under the waves near KHTX. The radar mosaic animation from this day shows precipitation associated with both the warm front and the dryline. Throughout the day, convective cells merged into squall lines which outran the dryline and eventually caught up with the warm front on 20 Mar. Fig. 9 shows the dryline retrograding to the west as the storms continue to propagate to the east at 0103 UTC 20 Mar. Little convection was present in association with the retrograding dryline because of the lack of daytime heating, which was assisting the parcels in reaching their LFC during the day.

a)

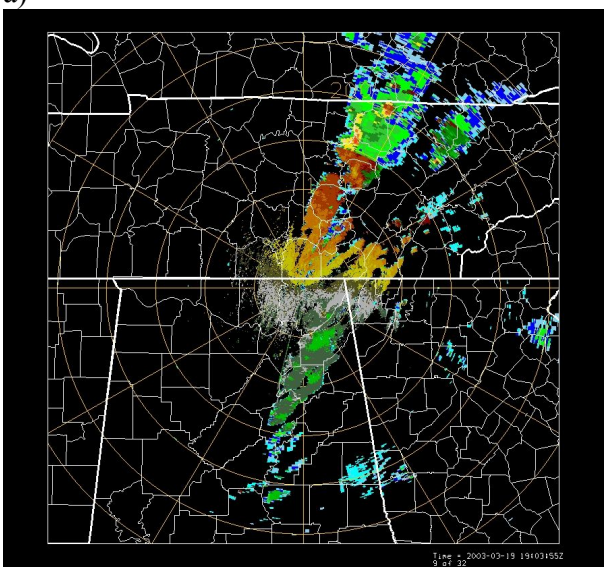

b)

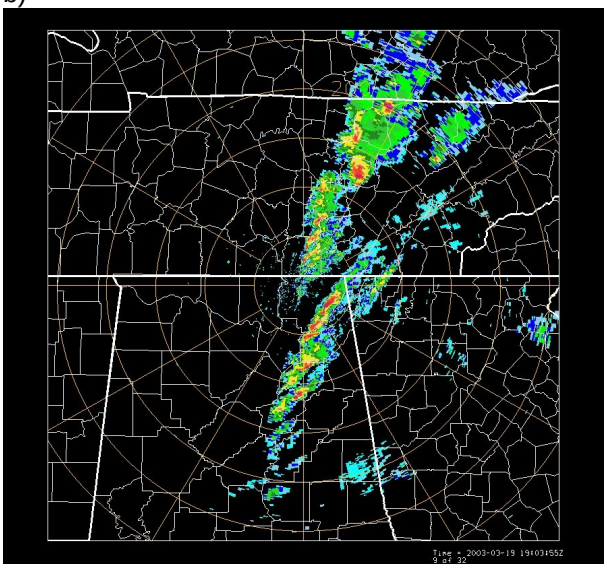

Fig. 8: WSR- 88D velocity (a) and reflectivity (b) data for 19 Mar at 1903 UTC taken from KHTX. The storms depict the dryline location and the velocity pattern shows the confluence and WAA in the region.

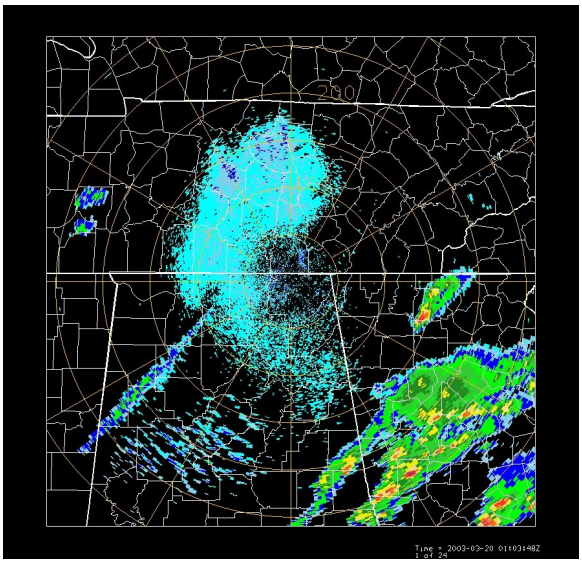

Fig. 9: Reflectivity data from KHTX on 20 Mar at 0103 UTC. The fineline shows the dryline's location. At this time, the dryline was retrograding across central AL while storms continued to propagate to the east.

6. MIPS DATA

Although most of the MIPS instruments were located east of the dryline, they provided an excellent depiction of the atmosphere during this event. The 915 MHz profiler provided fields of vertical motion, signal to noise ratio (SNR), and spectrum width (SW). The SNR time series for 19 Mar shows periods of heavy rain from 0700 to 0800 UTC, 2000 to 2100 UTC, and sporadically between 1000 and 1500 UTC. These periods of storms are indicated by SNR values of greater than 30 decibels (dB). The SW field shows high turbulence (values of up to 5.5 ms^{-1}) through much of the lowest four kilometers after 0700 UTC except for a two hour period between 0800 and 1000 UTC when SW values were low. The turbulence coincided with storms passing over Camp Adahi and also mixed the boundary layer, driving the dry air aloft toward the surface. However, the dryline did not reach the surface at camp Adahi since the MIPS did not analyze a substantial dewpoint drop in its surface data. The high SW values were confined to greater than .5 km AGL with very few exceptions at 1300 and 2200 UTC. The vertical wind profile at Camp Adahi shows that winds were unidirectional and southeasterly in the lowest .5 km, and then veered through a layer of about .8 km during times when no convective precipitation existed. The veering, which indicates WAA, suggests that the overrunning from the CAD was reaching Camp Adahi. During times of convective precipitation, winds backed in the boundary layer, suggesting the advection of rain- cooled air. In addition, downward vertical motion of greater than 5 ms^{-1} was recorded during the storms, indicating strong downdrafts. Otherwise, vertical motion was inconsistent due to high turbulence, as indicated by high SW values.

On 20 Mar, conditions did not favor dryline passage at Camp Adahi. SW values indicated a tranquil atmosphere except for a few shallow layers around 1000 UTC. The MIPS also reported downward vertical motion throughout the day. Convective precipitation is only apparent around 1000 UTC. The celiometer backscatter data and the bright band shown by the SNR profile show that the MIPS was located within a strataform cloud deck for much of the day. Fig. 10 shows that around 1000 UTC, winds started to weaken considerably in a layer from about .9 km to 1.7 km AGL. The convective boundary layer collapsed overnight and the wind direction changed from southeasterly to westerly within a layer of about 1 km. Since the winds are counteracting each other, a layer of very light southwesterly winds formed throughout this layer and persisted until about 1600 UTC. At this time the sun was able to heat the lower levels enough for the convective boundary layer to return and thus making the winds more uniform with height. Winds also backed at the surface due to the cold air drainage reaching Camp Adahi between 1200 and 1700 UTC and after 2100 UTC.

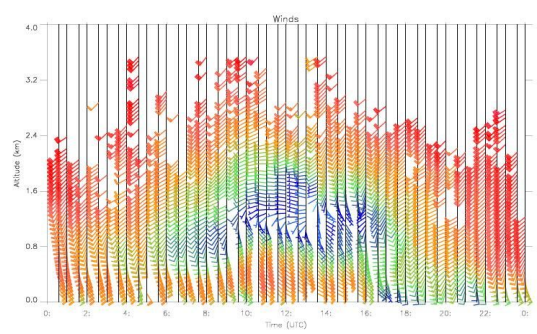

Fig. 10: 915 MHz wind profiler data from the MIPS over Camp Adahi on March 20th. This data shows a collapse in the convective boundary layer starting at 0630 UTC. A lull in the winds is observed at the height of the Appalachian Mountains as northeasterly winds blowing over the mountains from the Piedmont intersect with the southerly winds blowing into the region from the Gulf of Mexico. In addition, backing of the winds is observed at the surface in response to cold air drainage.

The MIPS radiometer was located on the roof of the NSSTC in Huntsville, AL during this event and was able to record atmospheric conditions to

10 km AGL. Precipitation ended around 1400 UTC 19 Mar, and low clouds persisted afterwards. Fig. 11 shows the radiometer data from 0100 UTC 19 Mar to 1743 UTC 20 Mar. Relative humidity (RH) readings on 19 Mar show a very moist middle troposphere from 0400 UTC until 1200 UTC. During much of this time, rain was falling over the city. The ambient temperature dropped from 1400 UTC to just before 1600 UTC in response to a shower. However, from just prior to 1600 UTC to 1700 UTC, it increased from 19 to 23° C. Over the same time period, RH values plummeted from near 100 % to about 50 %. The sharp coinciding increase in ambient temperature with a decrease in RH clearly shows dryline passage at this time. The air at the surface continued to become warmer and drier through 2200 UTC, at which the ambient temperature had approached 26° C and RH values had dropped to below 20 %. The corresponding dewpoint to the pre- dryline and post- dryline passages are 18.5° C and 1.3° C, respectively.

The time- height cross section shows maximum low- level heating corresponding with maximum drying while the dryline was east of the NSSTC. The higher temperatures on the dry side of the dryline occur because of the lower heat capacity of dry air. The pressure had been rising since Huntsville was well within the warm sector. No significant pressure fall is shown; however, the pressure trough associated with the dryline caused the pressure over the NSSTC to remain steady during the dryline passage. Fine- scale undulations in the pressure time series indicate gravity waves. The spike in the vertically integrated liquid time series of around 8 cm at 1500 UTC 19 Mar indicates the very moist column associated with the heavy precipitation that was falling over the NSSTC at this time.

The retrogression of the dryline became apparent on around 0100 UTC 20 Mar when daytime heating no longer played a role in the movement of the dryline. This caused the dewpoints to increase from about -1° C to 17° C in less than an hour. The ambient temperature simultaneously dropped from 24° C to 19° C from radiative cooling coupled with the virtual temperature ridge associated with the dryline moving farther to the west of Huntsville.

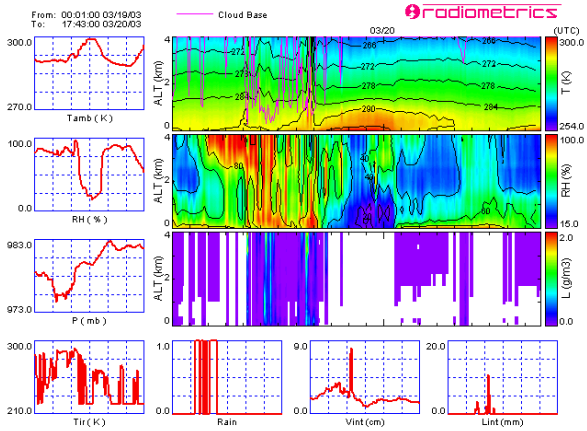

Fig. 11: MIPS radiometer data from 19-20 Mar 2003. Dryline passage is indicated by the simultaneous increase in ambient temperature and decrease in RH just before 1600 UTC 19 Mar. Dryline retrogression is noted by the sudden increase in RH around 0100 UTC 20 Mar. Clear to scattered sky conditions are recorded after the dryline passage, indicating very little active weather west of the dryline.

The time height RH cross section shows a moistening of the surface layer after the retrograding dryline passage to about 90%. The persistence of the moist surface layer responded to both the presence of the moist air to the east of the dryline and the dewpoint depression being less during the night, resembling the diurnal temperature cycle. The ambient temperature only dropped 4° C from the time of the retrograding dryline passage to sunrise (1200 UTC). At sunrise, the temperature started to rise again with the dewpoint staying relatively constant, causing the RH to decrease to 60% by 1730 UTC. This more closely resembles the diurnal temperature cycle and the data from the radiometer does not appear to indicate a second dryline passage over Huntsville. However, radiometer data was only available up to 1743 UTC and surface analyses from 20 Mar (Fig. 12) show a pronounced dewpoint gradient extending more northward as the day continues. In addition, a meteogram from KHSV shows a second dryline passage around 1700 UTC. The wind shifted from southeasterly to southwesterly and accelerated, enhancing mixing and thus propagating the dryline across central AL. Despite storms developing in the region, no precipitation fell over the NSSTC on 20 Mar.

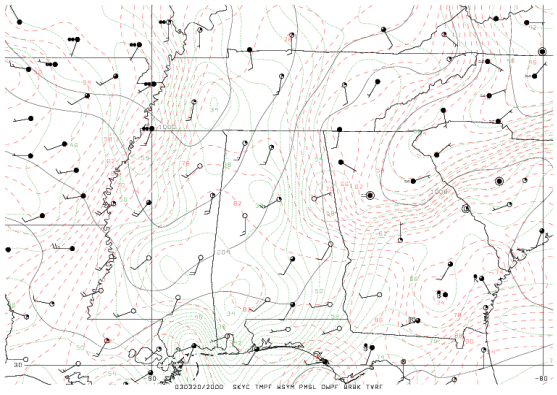

Fig. 12: As in Fig. 2 except for March 20th at 2000 UTC. This figure shows a dryline forming to the east of KHSV, between the MIPS and Camp Adahi, GA. The cold front can now be seen in central MS as the dryline persists in AL and CAD persists on the eastern side of the Appalachians.

7. CONCLUSION

This study documented and analyzed a dryline event east of the Mississippi River. On 19 Mar 2003, a dryline developed within the warm sector of an occluded mid-latitude cyclone and propagated across the southeast United States, mainly through AL. The synoptic pattern provided an excellent environment for large- scale lifting in this region and the dryline provided a region of enhanced moisture convergence. The SPC recognized the dryline and used it as an approximation for the edges of their convective outlook risk areas. Soundings for this region show a highly sheared environment with little CAPE, but the moisture convergence was enough to initiate a severe storm event which spawned 22 tornadoes. Soundings from east of the dryline show CAD occurring east of the Appalachians. The UAH MIPS, located at Camp Adahi, GA, also recorded the CAD in the vertical wind profile.

Data from the MIPS show that the dryline did not pass through Camp Adahi as the dryline intersected the air from east of the Appalachians and stalled between Huntsville, AL and Camp Adahi. The MIPS radiometer, which was left at the NSSTC in Huntsville, clearly shows the dryline passage at 1600 UTC 19 Mar. The dryline retrograded overnight and passed over the NSSTC at 0100 UTC 20 Mar while moving westward. It resumed its eastward motion during the day on 20 Mar and passed over the NSSTC at 1700 UTC. Using the MIPS and other tools, this rare weather phenomenon was able to be studied and presented.

8. FUTURE WORK

This study will be followed by a detailed duel-doppler radar analysis of a retrograding dryline during the International H_2O Project (IHOP, Weckworth et al 2004), of which documentation is also lacking in the literature. Documentations of different dryline events under different atmospheric conditions might provide better insight to causes of dryline motion and characteristics.

9. ACKNOWLEDGEMENTS

The author gratefully acknowledges Patrick Gatlin, Dustin Phillips, Wayne Mackenzie, Jr., Christopher Hain, Dr. Kevin Knupp, and Dr. John Mecikalski for their assistance with this study. In addition, the author gratefully acknowledges the NOAA Air Resources Laboratory (ARL) for the provision of the HYSPLIT transport and dispersion model and/or READY website (http://www.arl.noaa.gov/ready.html) used in this paper.

10. REFERENCES

Durran, D.R., and L.W. Snellman. 1987: The Diagnosis of Synoptic-Scale Vertical Motion in an Operational Environment. *Weather and Forecasting* **2:** 17-31.

Hane,C.E., M.E. Baldwin, H.B. Bluestein, T.M. Crawford, R.M Rabin. 2001: A Case Study of Severe Storm Development along a Dryline within a Synoptically Active Environment. Part I: Dryline Motion and an Eta Model Forecast. *Monthly Weather Review* **129.** 2183-2204.

Lindzen, R.S. and K.- K. Tung. 1976: Banded Convective Activity and Ducted Gravity Waves. *Monthly Weather Review* **104:** 1602- 1617.

McCarthy, J. and S.E. Koch. 1981: The Evolution of an Oklahoma Dryline. Part I: A Meso- and Subsynoptic-Scale Analysis. *Journal of the Atmospheric Sciences* **39:** 225-236.

Merritt, R.G. 2003: Radar Meteorology: MET 492. Class Textbook.

Parsons, D.B., M.A. Shapiro, R.M Hardesty, R.J. Zamora, J.M Intrieri. 1990: The Finescale Structure of a West Texas Dryline. *Monthly Weather Review* **119:** 1242-1258.

Peckham, S.E. and L.J. Wicker. 1999: The Influence of Topography and Lower-Tropospheric Winds on Dryline Morphology. *Monthly Weather Review* **128:** 2165-2189.

Rolph, G.D., 2003: Real-time Environmental Applications and Display sYstem (READY) Website. (http://www.arl.noaa.gov/ready/hplit4.html)

NOAA Air Resources Laboratory, Silver Spring, MD.

Sanders, F. and B.J. Hoskins. 1989: An Easy Method for Estimation of Q-Vectors from Weather Maps. *Weather and Forecasting* **5:** 346-353.

Schaefer, J.T. 1973: A Simulative Model of Dryline Motion. *Journal of the Atmospheric Sciences* **31:** 956-964.

Shaw, B.L., R.A. Pielke, C.L. Ziegler. 1996: A Three- Dimensional Numerical Simulation of a Great Plains Dryline. *Monthly Weather Review* **125:** 1489-1506.

Storm Prediction Center. 2004: Storm Reports page for 3/19/03. www.spc.noaa.gov.

Sun, W.Y. and Wu, C.C. 1991: Formation and Diurnal Variation of the Dryline. *Journal of the Atmospheric Sciences* **49:** 1606 1619.

Tollerud, E.I., F. Caracena, A. Marroquin, S. Koch, J.L. Moody, A. Wimmers. 2002: Relationships Between Dry Filaments and Mesoscale Convective Systems. *FSL Fourm.*

Uccellini, L.W. and S.E. Koch. 1987: The Synoptic Setting and Possible Energy Sources for Mesoscale Wave Disturbances. Monthly *Weather Review* **115:** 721- 729.

Weckwerth, T.M., D.B. Parsons, S.E. Koch, J.A> Moore, M.A. Lemone, B.B. Demoz, C. Flamant, B.Geerts, J. Wang, and W. F. Feltz, 2004: An Overview of the International H2O Project (IHOP_2002) and Some Preliminary Highlights. *Bulletin of the American Meteorological Society*, **85**: 253- 277.

Ziegler, C.L. and C.E. Hane. 1992: An Observational Study of the Dryline. *Monthly Weather Review* **121:** 1134-1151.

Ziegler, C.L., T.J. Lee, R.A. Pielke. 1996: Convective Initiation at the Dryline: A Modeling Study. *Monthly Weather Review* **125:** 1001-1026.